

Membrane waves and finite-frequency effects in surface wave tomography

Introduction

Full numerical integration of the equations of motion in 3D is expensive. The membrane wave method presented here simplifies it by restriction to two dimensions.

Membrane waves are used, as an analogue for Love and Rayleigh waves, to study surface wave propagation in the Earth. We present here new finite-difference software running on a Beowulf cluster which models finite-frequency effects (like scattering etc.) and compare our results with linear approximation theories.

Meshering of the Earth's surface

Discretization takes advantage of geodesic grids initially found for meteorological flow modelling.

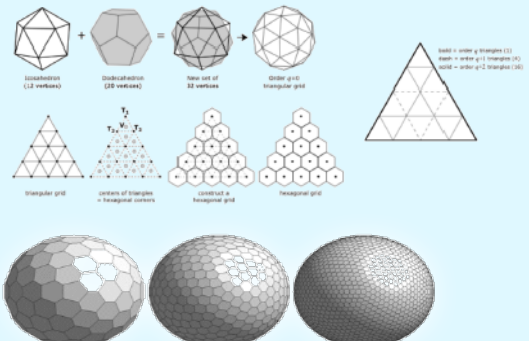


Fig. 1: Spherical grid construction uses initially the icosahedron & dodecahedron vertices. Refinement is done by subfolding corresponding triangles (Tape, 2003).

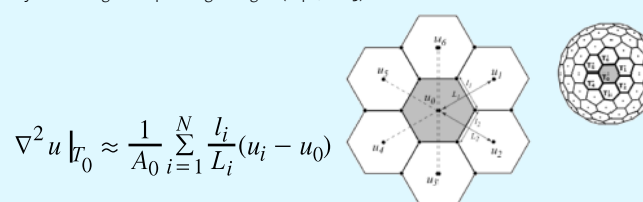


Fig. 2: Finite-difference scheme using cell area, center distances and cell edge lengths expresses the Laplacian on a spherical grid (Heikes&Randall, 1995; Tape, 2003).

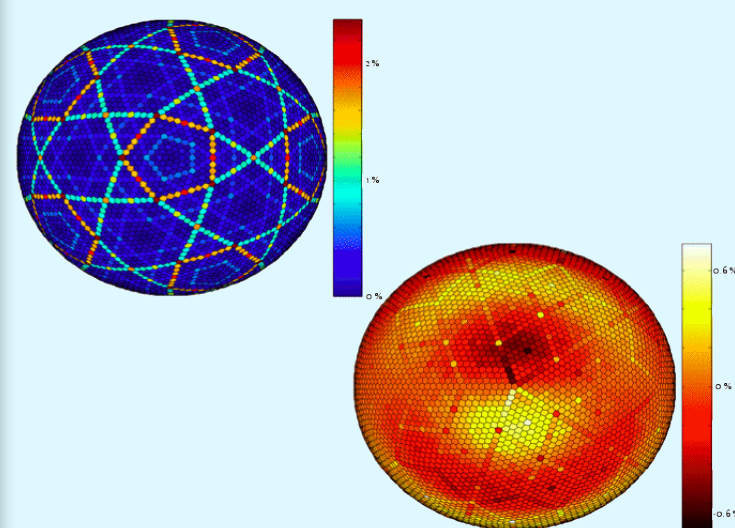


Fig. 3: Accuracy of Laplacian is influenced by grid distortion. Cell distortion on top is induced by the subfolding method. Differences to analytical solution for a spherical harmonic function ($L=6, M=1$) are still small compared to the maximum analytical Laplacian.

Membrane waves

$$(1) \rho \ddot{u} = \nabla \cdot \tau + f$$

$$(2) u_L = W(r)(-\hat{r} \times \nabla_\perp)\chi(\vartheta, \phi)$$

substituting Love wave ansatz (2) into (1) one finds that with smooth-Earth approximation χ obeys:

$$(3) \nabla_\perp^2 \chi = \omega^2 \chi$$

which is valid for each frequency ω (Tanimoto, 1990; Tromp & Dahlen, 1993). We solve (3) in time domain prescribing an initial displacement and "source time function":

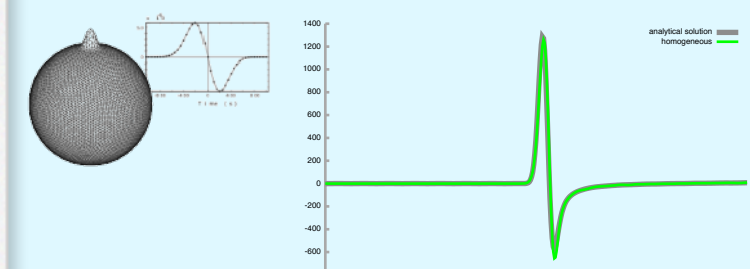


Fig. 4: Comparison can be made between analytical and numerical solution in the case of a homogeneous phase velocity map with a Gaussian initial displacement (in space and time shown on the left).

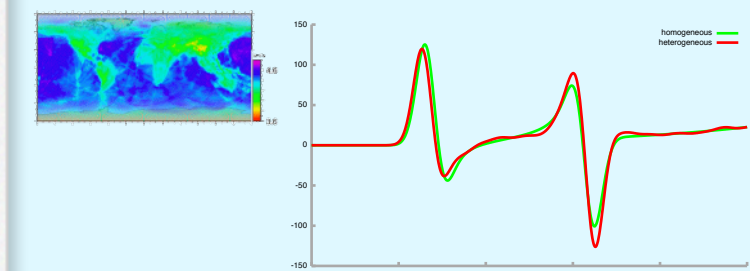


Fig. 5: Differences between solutions using a homogeneous vs. a heterogeneous phase velocity map (for Love waves at 35s).

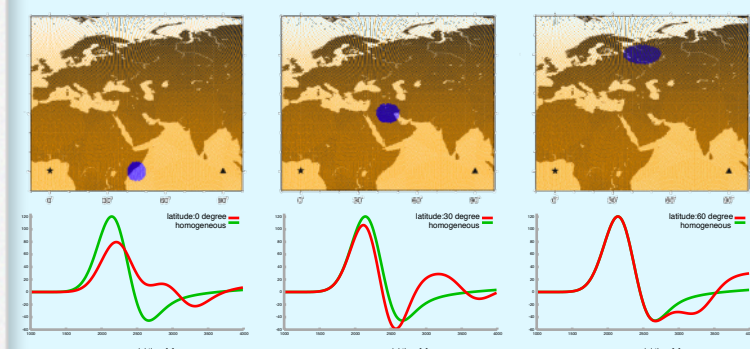


Fig. 6: Scattering effects for lateral heterogeneities (blue circles) depending on their location between source ($0^\circ/0^\circ$) and receiver ($0^\circ/90^\circ$).

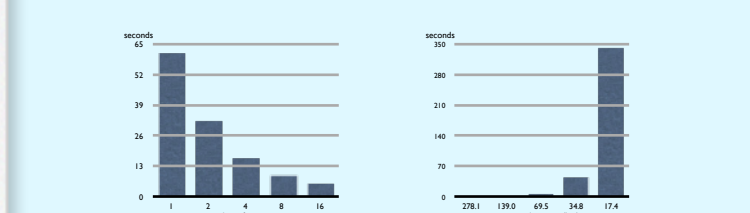


Fig. 7: Benchmarking of the code for Love waves at 150 s period with a propagation time of ~40 min. Calculation times are within seconds and scale well with respect to any cluster size.

Numerical sensitivity functions

Let us introduce the "Born" sensitivity function $K(\vartheta, \phi)$ such that

$$\delta\Phi = \int_{\Omega} K(\vartheta, \phi, \omega) \delta\nu(\vartheta, \phi, \omega) d\Omega$$

We perform a set of simulations with phase velocity

$$\delta\nu(\vartheta, \phi) = \begin{cases} 0 & \text{everywhere} \\ 1 & \text{within cell centered at } (\vartheta_i, \phi_i) \text{ and area } A_i \end{cases}$$

$\delta\Phi_i(\omega)$ is found by cross-correlation & filtering around ω . The Kernel values at each cell location are given by

$$\frac{\delta\Phi_i}{A_i} = K(\vartheta_i, \phi_i, \omega)$$

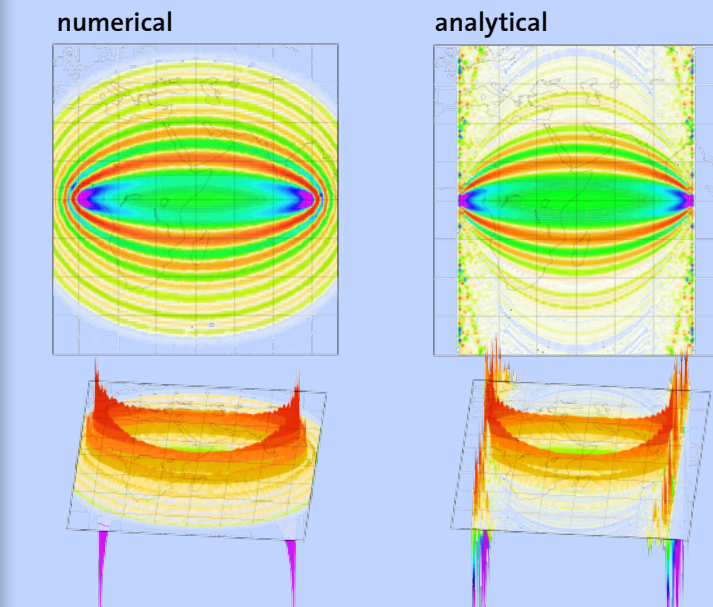


Fig. 8: Numerical finite-frequency sensitivity kernel for Love waves at 150 s period on the left compared to analytical one on the right (Spetzler et al., 2002).

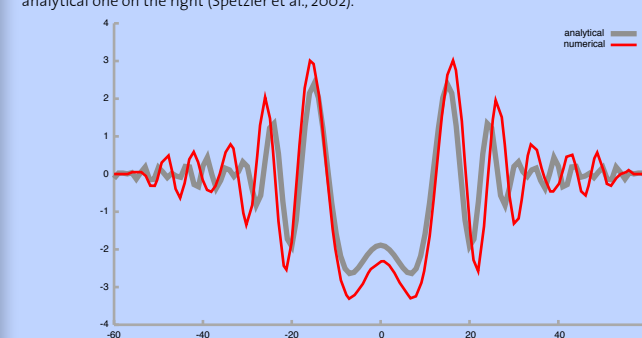


Fig. 9: Kernels of Fig. 8 plotted at 45° longitude, as a function of latitude.

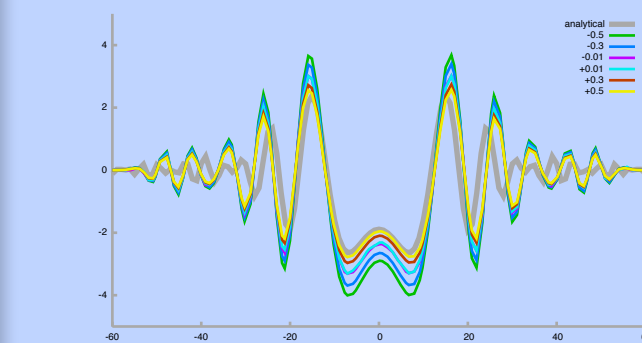


Fig. 10: Strange nonlinear effect: the kernel shape is effected by input values of $\delta\vartheta$. The kernel value converges for sufficiently small $\delta\vartheta$.

Numerical Integration vs. Linearized Theory

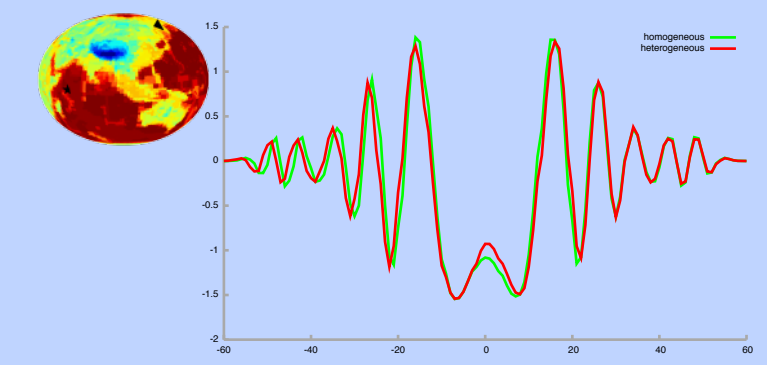


Fig. 11: Effects of a heterogeneous crustal phase velocity map (cross-section in the middle between a source at $0^\circ/60^\circ$ and a receiver at $60^\circ/150^\circ$ through the Tibetan anomaly)

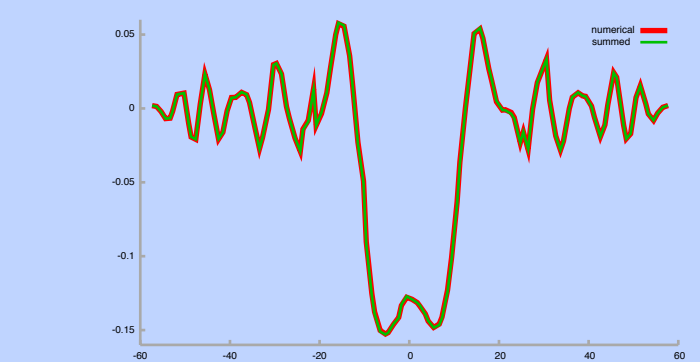


Fig. 12: Combined effect of two scatterers, modeled with a single simulation (red line) vs. two independent simulations whose results are then summed (green line). The experiment is repeated for ~100 couples of scatterers 5° degrees from each other; source and receiver are as in Fig. 6; all scatterers are at 45° longitude and $\delta\Phi$ is plotted as a function of latitude.

Conclusions

The membrane method allows for detailed investigations of various aspects of elastic wave propagation such as e.g. scattering & caustic effects, wavefront healing, focussing on a global scale.

3D (e.g. SEM) simulations of surface wave propagation take minutes even on large cluster systems (personal communication with Y. Capdeville); the same phenomena can be simulated within seconds by our 2D membrane wave software. Membrane waves are a very efficient tool to study finite-frequency effects in wave propagation.

In order to do tomography the next step will be to implement propagations with adjoint wavefields to further speed up the kernel calculations.

References:

- Heikes R, Randall DA, 1995. Numerical integration of the shallow-water equations on a twisted icosahedral grid. Part I: basic design and results of tests. Monthly Weather Review 123(6):1862-1880.
- Spetzler J, Trampert J, Snieder R, 2002. The effect of scattering in surface wave tomography. Geophys. J. Int., 149, 755-767
- Tanimoto T, 1990. Modelling curved surface wave paths: Membrane surface wave synthetics. Geophys. J. Int., 102, 89-100, 1990
- Tape C.H., 2003. Waves on a Spherical Membrane. Master thesis, University of Oxford.
- Tromp J, Dahlen F.A, 1993. Variational principles for surface wave propagation on a laterally heterogeneous Earth - III. Potential representation, Geophys. J. Int., 112, 195-209.

Acknowledgements:

Funding for this project is provided by Marie Curie Research Training Network SPICE. J. Woodhouse & C. Tape are thanked for their help & support.